A comparative study of the physical properties of Sb_2S_3 thin films treated with N_2 AC plasma and thermal annealing in N_2

M. Calixto-Rodríguez, H. Martínez, Y. Peña, O. Flores, H.E. Esparza-Ponce, A. Sanchez-Juarez, J. Campos-Álvarez, P. Reyes.

Abstract

As-deposited antimony sulfide thin films prepared by chemical bath deposition were treated with nitrogen AC plasma and thermal annealing in nitrogen atmosphere. The as-deposited, plasma treated, and thermally annealed antimony sulfide thin films have been characterized by X-ray diffraction (XRD), energy dispersive X-ray spectroscopy, scanning electron microscopy, atomic force microscopy, UV–vis spectroscopy, and electrical measurements. The results have shown that post-deposition treatments modify the crystalline structure, the morphology, and the optoelectronic properties of Sb_2S_3 thin films. X-ray diffraction studies showed that the crystallinity of the films was improved in both cases. Atomic force microscopy studies showed that the change in the film morphology depends on the postdeposition treatment used. Optical emission spectroscopy (OES) analysis revealed the plasma etching on the surface of the film, this fact was corroborated by the energy dispersive X-ray spectroscopy analysis. The optical band gap of the films (E_g) decreased after post-deposition treatments (from 2.36 to 1.75 eV) due to the improvement in the grain sizes. The electrical resistivity of the Sb_2S_3 films decreased from 10^8 to 10^6 Ω-cm after plasma treatments.

Keywords: Sb_2S_3, Thi film, Plasma treatment, Chemical bath deposition.

Experimental details

Deposition of thin films: Sb_2S_3 thin films were prepared using the chemical bath deposition technique, following the procedure reported by Nair et al. [17]. The bath was prepared using antimony trichloride ($SbCl_3$) and sodiumthiosulfate ($Na_2S_2O_3$) as follows: In a 100ml beaker, we have used 721 mg instead of 650 mg of $SbCl_3$ which was dissolved in 2.5 ml of acetone. To this mixture was added 25 ml of sodium thiosulfate 1 M followed by 72.5 ml of deionized cold water (both maintained ~10 °C) and stirred well. Borosilicate microscope glass slides from Corning with dimensions of 7.5 cm x 2.5 cm x 0.1 cm were used as substrates. The substrates were placed vertically in the solution. The deposition was made at ~10 °C for 4 h without stirring. At the end of the deposition the slides, coated on both sides with orange yellow films, were removed from the bath, washed well with distilled water, and dried with a constant flow of air. The coating deposited on the side of the substrate facing the wall of the beaker was retained for nitrogen plasma treatments and thermal annealing in nitrogen atmosphere. The coating on the other side was wiped off with dilute acid. Thickness of the films was measured using an Alpha Step model 100 profilometer from Tencor Instruments. Typical thickness obtained for as-deposited films was 385 nm, while for films after nitrogen plasma treatment and thermal annealing in nitrogen atmosphere were 311 and 260 nm, respectively.

Post-deposition treatments of antimony sulfide thin films: The experimental apparatus and technique to generate the pulsed plasma was recently reported [19,20]. A brief description is reported here. The discharge chamber used in this work has two stainless steel circular plate electrodes, 1 mm thick and 30 mm in diameter. The electrodes are positioned horizontally at the center of the reaction chamber with 4 mm

of separation between them. Samples were placed on the bottom electrode. The N_2 gas was injected into the reaction chamber through the front flange. The same gas connection was used for pressure sensor. The discharge power supply was maintained at an output of 300 V and a current of 0.36 A. The base pressure of the reaction chamber was maintained at 3.0 x 10^{-2} Torr using a mechanical pump (Varian SD-301) and purged with nitrogen at 1.0 Torr for several times in order to remove the background gases. The as-deposited antimony sulfide thin films were treated with nitrogen plasma at 3.0 Torr during 60 min.

For the as-deposited antimony sulfide thin films, a thermal treatment in nitrogen atmosphere at 300 8C and 300 mTorr during 60 min was undertaken, which was performed in an oven with temperature and pressure controls. The as-deposited, plasma treated, and thermally annealed thin films were structurally, compositionally, morphologically, optically and electrically characterized.

Characterization: XRD diffraction patterns were recorded on a Rigaku D-Max Xray diffractometer using Cu-K_α radiation (λ = 1.5406 Å). The chemical composition of the as-deposited, plasma treated, and thermally annealed antimony sulfide thin films was determined by energy dispersive X-ray spectroscopy (EDS) using an Inca Oxford Instruments system attached to the scanning electron microscope (SEM). The surface morphology was studied by scanning electron microscopy (SEM) JEOL model JSM 5800LV at 15 kV and 10,000x. Atomic force microscopy (AFM) analysis was done using a Nanosurf EasyScan E-line equipment, the topography contrast images were acquired in the contact mode. For the optical emission spectroscopy (OES) analysis, an optic fiber was connected to the entrance aperture of a high-resolution Ocean Optics Inc.

Spectrometer Model HR2000CG-UV-NIR, equipped with a 3 x 10^5 lines-m^{-1} composite blaze grating and a UV2/OFLV-5 detector (2048-element linear silicon CCD array). The grating response has a spectral response in the range of 200–1100 nm with efficiency >30%. The optical transmittance at normal incidence, and specular reflectance spectra of the samples were measured with a spectrophotometer Shimadzu model UV-1601PC in the UV–vis–NIR region (190–1100 nm wavelength range). For the electrical measurements, current versus time data were recorded on an automated system using a Keithley 619 electrometer and a Keithley 230 programmable voltage source. A pair of coplanar silver print electrodes of 3 mm in length, 3 mm in separation, was applied on the surface of the films.

Results and discussion

X-ray diffraction (XRD) and compositional analyses: Fig. 1 shows the X-ray diffraction (XRD) patterns for asdeposited, plasma treated, and thermally annealed antimony sulfide thin films. No diffraction peaks were observed in the XRD pattern of the as-deposited thin film, indicating that the deposited material is either amorphous or of poor crystallinity. It is a common result for as-prepared antimony sulfide thin films obtained by the chemical bath deposition method [21–24]. The diffraction patterns corresponding to films after nitrogen plasma treatment, and thermal annealing match well the standard for Sb_2S_3 (JCPDS 42-1393) which has an orthorhombic structure. The XRD pattern of the Sb_2S_3 thin film after thermal annealing showed peaks higher than those obtained for film treated with nitrogen plasma, with a preferential orientation along the (3 1 0) direction. The mean value of the crystallite sizes for the Sb_2S_3 thin films treated with nitrogen plasma and films thermally annealed were calculated for the

diffraction peak oriented in the direction (3 1 0) using the Scherrer formula D = (0.9λ)/(βcos θ), where D is the diameter of crystallites, λ is the wavelength of CuKα line, β is full width at half maximum (FWHM) in radians and u is Bragg's angle. The mean crystallite size for the plasma treated film was 13.7 nm, and for the film thermally annealed was 19.1 nm. The nitrogen plasma and thermal treatments improved the crystalline structure of the as-deposited antimony sulfide thin films.

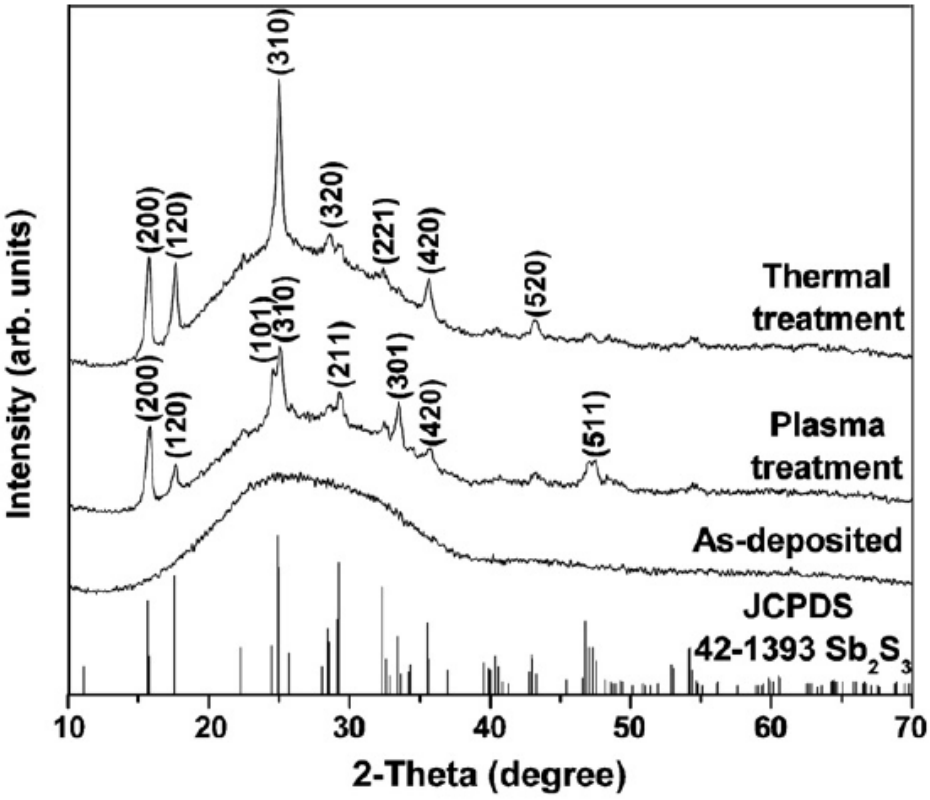

Fig. 1. X-ray diffraction patterns for as-deposited, plasma treated, and thermally annealed antimony sulfide thin films.

Table 1
Chemical composition of antimony sulfide thin films by EDS.

Sample	Sb (at%)	S (at%)
As-prepared	46.54	53.46
Plasma treated	45.50	54.50
Thermally treated	46.70	53.30

Table 1 shows the chemical composition in atomic percent (at%) for as-deposited, plasma treated, and thermally annealed antimony sulfide thin films. The chemical composition on asdeposited films was: 53.46% for S and 46.54% for Sb, this suggests that the as-deposited films are close to the Sb2S3 stoichiometric composition. The decrease in the antimony content obtained for the film after plasma treatment might be due to the plasma etching of this element on the surface of the film. The little decrease in the sulfur content obtained for film after thermal annealing is probably due to the loss of sulfur during the annealing process.

Morphological analysis: Fig. 2 shows typical SEM pictures of the morphology of (a) asdeposited, (b) thermally annealed, and (c) plasma treated antimony sulfide thin films. There are no significant changes in the morphology for the as-deposited and plasma treated films. The morphology in the thermally annealed film looks very smooth. In the three cases there are clusters of quasi-spherical shape and varying size. The mean grain sizes of these clusters on the surface of the as-deposited, plasma treated, and thermally annealed films are 249, 313, and 359 nm, respectively.

Fig. 3 shows typical AFM images of the surface topography in 3D for the antimony sulfide thin films: (a) the as-deposited film is formed by very small grains; (b) the thermally annealed film shows that the small grains had coalesced because of the

annealing temperature, resulting in a uniform surface with some additional big grains observed on the film surface; and (c) for plasma treated film, the surface is uniform and smoother than those observed in the other conditions. The root mean square (rms) value for asdeposited film is 6.7 nm, meanwhile the rms values are modified for thermally annealed and plasma treated films. The rms for thermally annealed film was 8.1 nm, this increase in the roughness is induced by the cluster growth. The value of the roughness for the film after plasma treatment was lower (6.0 nm) compared to that obtained for the as-deposited film. This may be due to the erosion of the film during the plasma process.

Optical emission spectroscopy (OES) analysis: The interaction of the nitrogen plasma and the surface of antimony sulfide thin film allows the generation of new species in the plasma. To identify these species, OES measurements were carried out during the experiments. Fig. 4 shows a typical optical emission spectrum for the plasma. The measurements allowed the analysis of the most luminous area that corresponds to the negative glow near the cathode dark space. The identified species from the Sb2S3 film–nitrogen plasma interaction were: N_2 at 235.14nm ($D^3\Sigma_u^+$-$B^3\Pi_g$), 246.16nm ($A^3\Sigma_u^+$-$^1\Sigma_g^+$), 280.46, 295.32, 297.68, 313.60, 315.93, 337.13, 353.67, 370.62, 380.49, 399.84, 405.94, and 434.36 ($C^3\Pi_u$-$B^3\Pi_g$); N_2^+ at 334.96, and 375.61 ($B^2\Sigma_u^+$-$X^2\Sigma_g^+$); NS at 246.56 ($A^2\Delta$-$X^2\Pi$), 258.48 ($A^2\Delta$-$X^2\Pi$), 258.70 ($C^2\Sigma$-$X^2\Pi$), 269.74 ($A^2\Delta$-$X^2\Pi$), 419.17 ($B^2\Pi$-$X^2\Sigma$); S_2 at 269.76 ($f^1\Delta u$-$a^1\Delta_g$), 313.22, 355.56, 358.72, 393.89, 419.36, and 456.30 ($B^3\Sigma_u^-$-$X^3\Sigma_g^-$); and SbS at 380.87, 399.18, 413.68, and 448.73 [25,26]. The majority of the species are vibrationally excited. S_2 and SbS species were detected in the plasma, the origin of

these species is from the film surface, so plasma treatment changed the chemical composition of the Sb2S3 film as revealed by the EDS analysis.

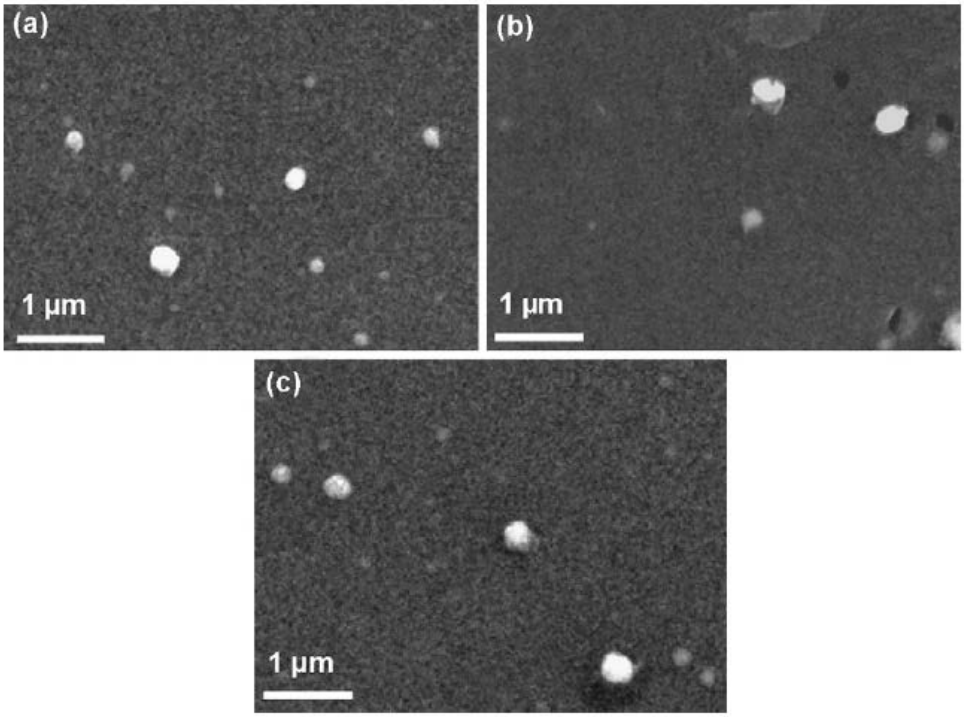

Fig. 2. SEM images for (a) as-deposited, (b) thermally annealed, and (c) plasma treated antimony sulfide thin films.

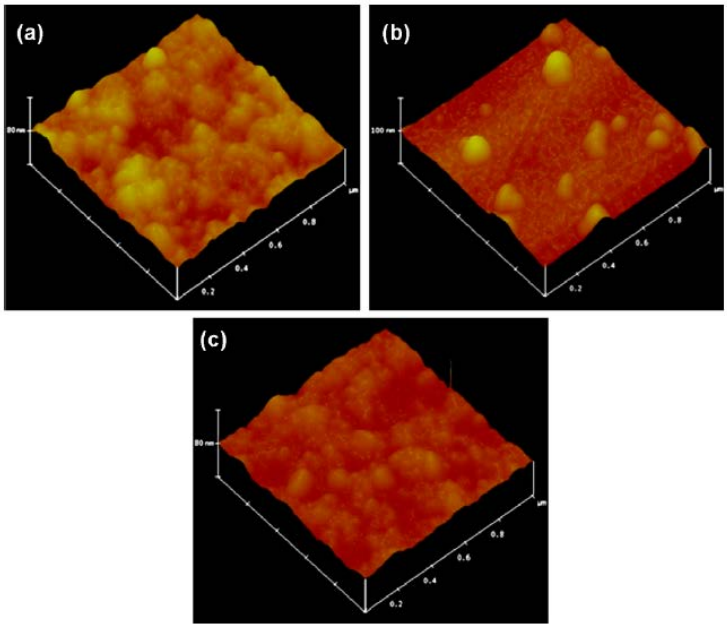

Fig. 3. AFM images for (a) as-deposited, (b) thermally annealed, and (c) plasma treated antimony sulfide thin films.

Optical and electrical properties: Fig. 5a–c shows the behavior of the optical transmittance T(λ) and specular reflectance R(λ) spectra for as-deposited, plasma treated, and thermally annealed antimony sulfide thin films. The as-prepared films are transparent at wavelengths, λ > 526 nm. A shift in the absorption edge toward larger wavelength is observed for plasma treated and thermally annealed films. The values of the absorption coefficient α(λ) for the as-deposited, plasma treated, and thermally annealed films were calculated from the data obtained from the transmission T, reflection R, and thickness d, using the well-known relationship [27]

$$T = \frac{(1-R)^2}{\exp(\alpha d) - R^2 \exp(-\alpha d)}. \qquad (1)$$

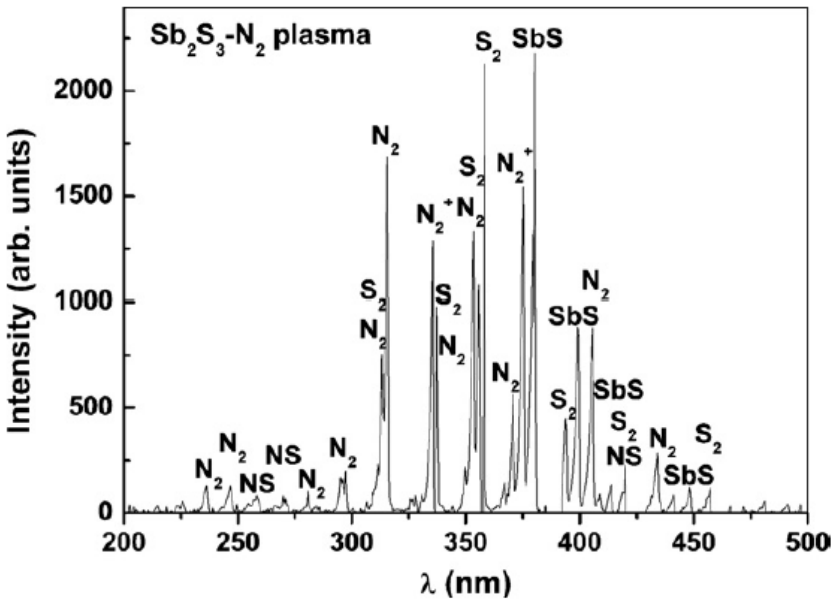

Fig. 4. Typical OES spectrum for nitrogen plasma-Sb_2S_3 thin film interaction.

For allowed direct transitions, αhv is given by [28]

$$(\alpha h\nu)^2 = A(h\nu - E_g), \qquad (2)$$

where A is a constant and E_g is the optical band gap. Thus E_g can be obtained from a plot of $(\alpha hv)^2$ versus hv. The E_g values were calculated from the best fit of the plot $(\alpha hv)^2$ versus hv, and its extrapolation to $(\alpha hv)^2 = 0$ (see Fig. 6). The as-deposited antimony sulfide thin film has a band gap of 2.36 eV. The E_g values for plasma treated and thermally annealed Sb2S3 films were 1.83 and 1.75 eV, respectively. A higher band gap for the as-deposited film (2.36 eV versus 1.75 eV for thermally annealed films) is attributed to size quantization as explained by Nair et al. [17] and Salem and Selim [29] for chemically deposited antimony sulfide thin films. The reduction in the band gaps of the films after post-deposition treatments is ascribed to the improvement in the crystallinity, which is evidenced in the XRD patterns given in Fig. 1.

The electrical resistivity (ρ) value for the as-deposited thin film was 6.2×10^8 Ω-cm. The ρ values for plasma treated and thermally annealed Sb_2S_3 thin films were 4.5×10^6 and 5.3×10^8 Ω-cm, respectively. A ρ value of 10^8 Ω-cm was reported by Cardenas et al. [30] for chemically deposited antimony sulfide thin films after annealing in nitrogen at 300 °C. Although, films after thermal treatment had better crystalline structure compared to as-deposited films, it was not observed a decrease in its electrical resistivity. Films after plasma treatment showed a reduction in the electrical resistivity in two orders of magnitude, this might be due to the etching at the film surface. The etching at the film surface in the plasma treatment improved the electrical transport at the surface. Note that the electrical measurements were done on the surface of the

films in the planar configuration. It was unable to measure the conductivity type using the hot point probe technique in these samples because of its high electrical resistivity.

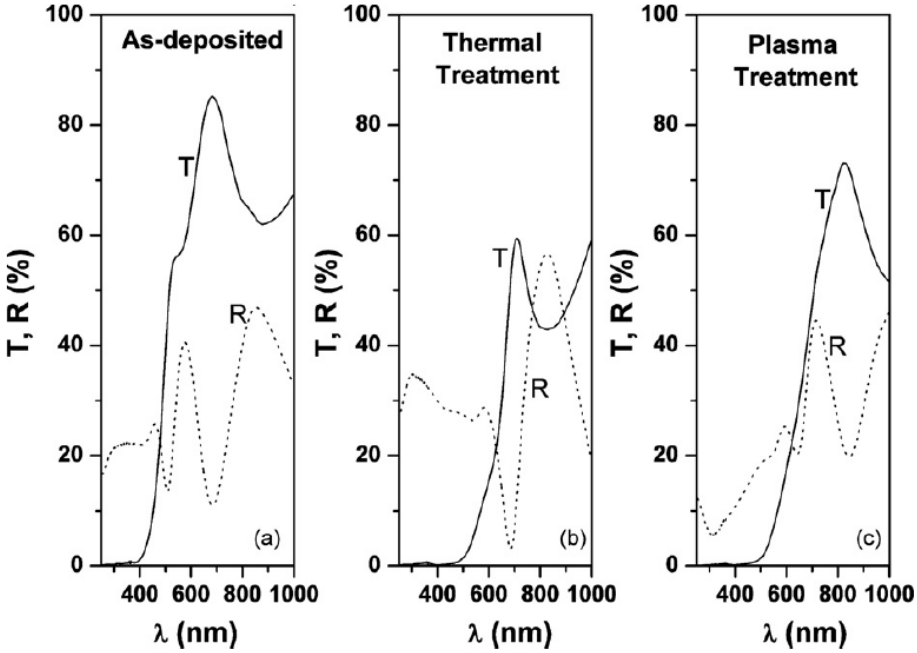

Fig. 5. $T(\lambda)$ and $R(\lambda)$ for as-deposited, thermally annealed, and plasma treated antimony sulfide thin films.

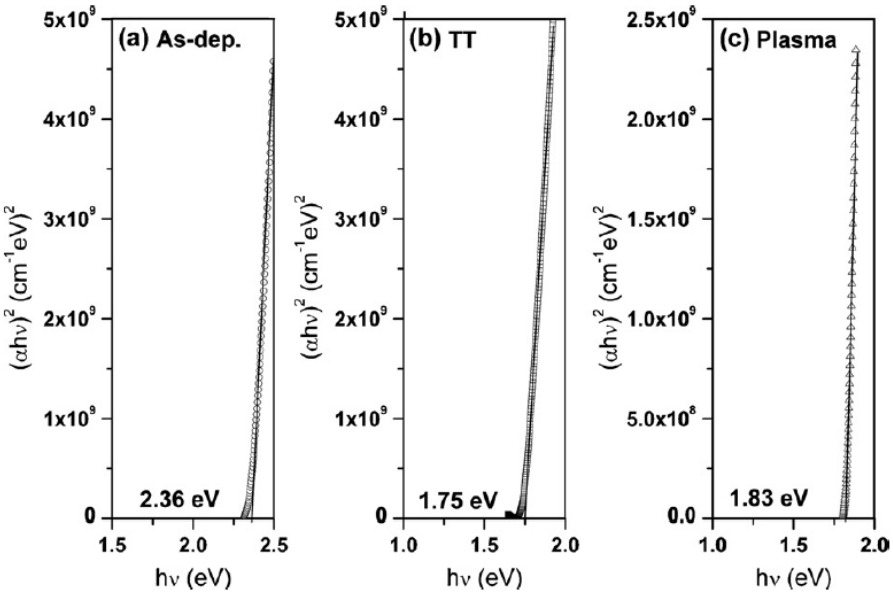

Fig. 6. Plots of $(\alpha h\nu)^2$ versus $h\nu$ for as-deposited, thermally annealed, and plasma treated antimony sulfide thin films.

Conclusions

Antimony sulfide thin films chemically depositedwere treated in nitrogen plasma and thermal annealing in nitrogen atmosphere to compare their structural, optical and electrical properties after the post-deposition treatments. XRD results revealed that the best crystallization of the films was obtained by thermal annealing. The E_g values for plasma treated and thermally annealed antimony sulfide thin films were 1.83 and 1.75 eV, respectively. Films after thermal annealing in nitrogen atmosphere did not show any change in the electrical resistivity value (10^8 Ω-cm). Films after plasma treatment showed a reduction in the electrical resistivity from 10^8 to 10^6 Ω-cm. Plasma treatments can be used to improve the electrical properties of as-deposited Sb_2S_3 thin films.

Acknowledgements

The authors are thankful to Maria Luisa Ramón for the XRD measurements (CIE-UNAM), José Ortega (CIE-UNAM) and A. González (ICF-UNAM) for technical support, M.T.S. Nair and P.K. Nair (CIE-UNAM) for providing some experimental facilities, and M.E. Calixto for valuable discussions. One of the authors (MCR) acknowledges the financial support received from DGAPA-UNAM. This research was partially sponsored by DGAPA IN-105707-3, DGAPA IN 111506, and CONACyT 41072-F.

References

[1] M.J. Chockalingam, K.N. Rao, N. Rangarajan, C.V. Suryanarayana, Studies on sintered photoconductive layers of antimony trisulphide, J. Phys. D: Appl. Phys. 3 (1970) 1641–1644.

[2] E. Montrimas, A. Paz˘era, Charge carrier transport and space charge in thin films of antimony trisulphide, Thin Solid Films 34 (1976) 65–68.

[3] J. George, M.K. Radhakrishnan, Electrical conduction in coevaporated antimony trisulphide films, Solid State Commun. 33 (1980) 987–989.

[4] K.Y. Rajpure, C.H. Bhosale, (Photo)electrochemical investigations on spray deposited n-Sb2S3 thin film/polyiodide/C photoelectrochemical solar cells, Mater. Chem. Phys. 63 (2000) 263–269.

[5] Y. Rodrı´guez-Lazcano, M.T.S. Nair, P.K. Nair, Photovoltaic p-i-n structure of Sb2S3 and CuSbS2 absorber films obtained via chemical bath deposition, J. Electrochem. Soc. 152 (2005) G635–G638.

[6] K. Bindu, M.T.S. Jose´ Campos, A. Nair, P.K. Sa´nchez, Nair, Semiconducting AgSbSe2 thin film and its application in a photovoltaic structure, Semicond. Sci. Technol. 20 (2005) 496–504.

[7] K. Bindu, M.T.S. Nair, T.K. Das Roy, P.K. Nair, Chemically deposited photovoltaic structure using antimony sulfide and silver antimony selenide absorber films, Electrochem. Solid-State Lett. 9 (2006) G195–G199.

[8] S. Messina, M.T.S. Nair, P.K. Nair, Antimony sulfide thin films in chemically deposited thin film photovoltaic cells, Thin Solid Films 515 (2007) 5777–5782.

[9] A. Arato, E. Ca´ rdenas, S. Shaji, J.J. O'Brien, J. Liu, G. Alan Castillo, T.K. Das Roy, B. Krishnan, Sb2S3:C/CdS p-n junction by laser irradiation, Thin Solid Films 517 (2009) 2493–2496.

[10] K. Bindu, M.T.S. Nair, P.K. Nair, Chemically deposited Se thin films and their use as a planar source of selenium for the formation of metal selenide layers, J. Electrochem. Soc. 153 (2006) C526–C534.

[11] R. Sagar, M.P. Srivastava, Amorphization of thin film of CdS due to ion irradiation by dense plasma focus, Phys. Lett. A 183 (1993) 209–213.

[12] Z.Y. Zhong, Y.D. Jiang, Surface modification and characterization of indium-tin oxide for organic light-emitting devices, J. Colloid Interface Sci. 302 (2006) 613–619.

[13] G. Lavareda, C. Nunes de Carvalho, A. Amaral, E. Fortunato, P. Vilarinho, a-Si:H TFT enhancement by plasma processing of the insulating/semiconductor interface, Mater. Sci. Eng. B 109 (2004) 264–268.

[14] P. Arun, A.G. Vedeshwar, Laser induced crystallization in Sb2S3 films, Mater. Res. Bull. 32 (1997) 907–913.

[15] R.K. Debnath, A.G. Fitzgerald, Electron beam induced surface modification of amorphous Sb2S3 chalcogenide films, Appl. Surf. Sci. 243 (2005) 148–150.

[16] I. Grozdanov, A simple and low-cost technique for electroless deposition of chalcogenide thin films, Semicond. Sci. Technol. 9 (1994) 1234–1241.

[17] M.T.S. Nair, Y. Pen˜ a, J. Campos, V.M. Garcia, P.K. Nair, Chemically deposited Sb2S3 and Sb2S3-CuS thin films, J. Electrochem. Soc. 145 (1998) 2113–2120.

[18] B. Krishnan, A. Arato, E. Cardenas, T.K. Das Roy, G.A. Castillo, On the structure, morphology, and optical properties of chemical bath deposited Sb2S3 thin films, Appl. Surf. Sci. 254 (2008) 3200–3206.

[19] M. Calixto-Rodriguez, H. Martı´nez, A. Sanchez-Juarez, AC plasma induced modifications in b-In2S3 thin films prepared by spray pyrolysis, Thin Solid Films 517 (2009) 2332–2334.

[20] H. Martínez, F.B. Yousif, Electrical and optical characterization of pulsed plasma of

N2–H2, Eur. Phys. J. D 46 (2008) 493–498.

[21] K.C. Mandal, A. Mondal, A new chemical method for preparing semiconductor grade antimony tri-sulphide thin films, J. Phys. Chem. Solids 51 (1990) 1339–1341.

[22] O. Savadogo, K.C. Mandal, Studies on new chemically deposited photoconducting antimony trisulphide thin films, Sol. Energy Mater. Sol. Cells 26 (1992) 117–136.

[23] I. Grozdanov, A simple and low cost technique for electroless deposition of chalcogenide thin films, Semicond. Sci. Technol. 9 (1994) 1234–1241.

[24] C.D. Lokhande, B.R. Sankapal, R.S. Mane, H.M. Pathan, M. Muller, M. Giersig, V. Ganesan, XRD, SEM, AFM, HRTEM, EDAX and RBS studies of chemically deposited Sb2S3 and Sb2Se3 thin films, Appl. Surf. Sci. 193 (2002) 1–10.

[25] R.W.B. Pearse, A.G. Gaydon, The Identification of Molecular Spectra, University Printing House Cambridge, Great Britain, 1976.

[26] http://physics.nist.gov/PhysRefData/Handbook/element_name.htm.

[27] T.S. Moss, Optical Properties of Semiconductors, Butterworths, London, 1959.

[28] K.L. Chopra, S.R. Das, Thin Film Solar Cells, Plenum Press, New York, 1983.

[29] A.M. Salem, M.S. Selim, Structure and optical properties of chemically deposited Sb2S3 thin films, J. Phys. D: Appl. Phys. 34 (2001) 12–17.

[30] E. Cardenas, A. Arato, E. Perez-Tijerina, T.K. DasRoy, G. AlanCastillo, B. Krishnan, Carbon-doped Sb2S3 thin films: structural, optical and electrical properties, Sol. Energy Mater. Sol. Cells 93 (2009) 33–36.